

NICHOLAS P. TALICEO, DANIEL A. GRIFFITH

University of Texas at Dallas, USA

THE K_4 GRAPH AND THE INERTIA OF THE ADJACENCY MATRIX FOR A CONNECTED PLANAR GRAPH

Abstract: The K_4 graph and the inertia of the adjacency matrix for a connected planar graph. A substantial history exists about incorporating matrix analysis and graph theory into geography and the geospatial sciences. This study contributes to that literature, aiding in analyses of spatial relationships, especially in terms of spatial weights matrices. We focus on the n -by- n 0–1 binary *adjacency matrix*, whose rows and columns represent the nodes of a connected planar graph. The inertia of this matrix represents the number of positive (n^+), negative (n^-), and zero (n^0) eigenvalues. Approximating the Jacobian term of spatial auto-normal models can benefit from calculating these matrix quantities. We establish restrictions for n exploiting properties we uncover for the K_4 graph.

Keywords: K_4 graph, planar graph, matrix inertia, adjacency matrix, Jacobian term

JEL codes: C4, C6

1. Introduction

The relevant problem involves the estimation of the Jacobian term, J , of the likelihood function, L , for an auto-normal (-Gaussian) random variable, such that

$$L = J \cdot f(\rho, \beta, \sigma^2), \quad (1)$$

where

$$J = \pi \prod_{i=1}^n (1 - \lambda_i)^2, \quad (2)$$

f represents the likelihood equation for either the autoregressive response (AR), conditional autoregressive (CAR), or simultaneous autoregressive (SAR) model, ρ

is the spatial autocorrelation parameter $\frac{1}{\lambda_{min}} \leq \rho \leq 1$, β is a $(k + 1) \times 1$ vector of

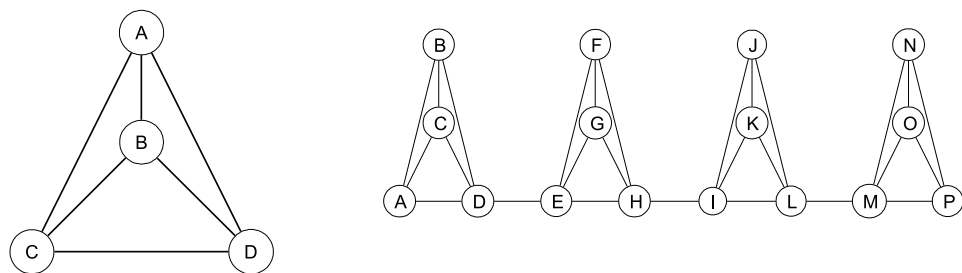
regression coefficients, and σ^2 is the variance of the attribute distribution under study [Bivand et al. 2013].

Estimation of Equation (1) employs the use of graph theory and matrix analysis, specifically in the determination of the eigenvalues (λ_i) for the Jacobian term. For an undirected, connected, and planar graph, one can compute the $n \times n$ adjacency matrix (\mathbf{A}), also known as a 0–1 binary spatial weights matrix, by representing a link between two nodes (e.g., a common areal units boundary) i and j with a value of 1, and a 0 if no such link exists. Next, one can calculate the inertia of matrix \mathbf{A} , a tuple of values that represents the number of positive, negative, and zero eigenvalues (n^+, n^-, n^0), respectively). These results from the inertia calculation then can be used to calculate an approximation of J for the preceding likelihood function given by Equation (1).

We are re-evaluating a previously conjectured upper bound for the percentage of n^- [Griffith, Luhanga 2011], which, generally speaking, states that the percentage of negative eigenvalues of the inertia for some undirected, connected, planar graph with n nodes has a maximum value of $\frac{2}{3}n$. Since the positing of this conjecture, a counterexample has been highlighted [Elphick, Wocjan 2016], which is for an unrealistically small value of n . This counterexample is known as the K_4 connected planar graph, and is illustrated in Figure 1a.

Because of a reliance on the K_4 graph, most likely a limited number of cases do not follow the conjecture proposed by Griffith and Luhanga [2011]. Moreover, all graphs that are inconsistent with this conjecture appear to contain one or more K_4 subgraphs.

The Jacobian term allows for the implementation of Gaussian SAR models for massive n . Due to equations outlined in Griffith [2015], which provide good eigenvalue approximations for regular square tessellations when n is in the millions, estimations of the Jacobian term are straightforward; cases of large n include data collected from remotely-sensed images. However, the equations outlined in Griffith [2015] do not hold for irregular surface partitionings, requiring other formulations to calculate their Jacobian terms. By creating a bound for the percentage of n^- for the inertia of a connected planar graph, one is improving the estimation of the auto-normal model for irregular surface partitionings by making more accurate the estimation of eigenvalues in the Jacobian term J in Equation (2).



a) The K_4 complete planar graph,

b) A chain of K_4 subgraphs, with each sequential pair connected by a single link

Fig. 1. Two selected counterexamples to the Griffith and Luhanga [2011] conjecture

Our goal is to determine the implications of existing K_4 subgraphs in graphs of interest; i.e., spectra of graphs containing K_4 subgraphs, K_4 subgraph tessellations, and empirical examples. We initiate our discussion by examining a variety of specimen graphs, and determining their overall properties. We also report results from simulation experiments.

1.1. A Numerical Illustration

To illustrate the effects of eigenvalue approximations on Jacobian approximations, we use a graph spectrum with a known percentage of negative eigenvalues that is constant at 75 percent. The graph used to illustrate these approximations is illustrated in Figure 1b, where each K_4 subgraph is connected to its immediate neighbor by a single link.

The eigenvalues of a 0–1 spatial weights matrix (denoted by \mathbf{C} in that literature) and its row-standardized counterpart (matrix \mathbf{W}), result in the following values:

$$y_i = \frac{\lambda_i - \lambda_{\min}}{\lambda_{\max} - \lambda_{\min}} \in [0; 1] \text{ or } y_i = \frac{\lambda_i - \lambda_{\min}}{1 - \lambda_{\min}} \in [0; 1]$$

$$\Rightarrow \bar{y} = \mu = \frac{-\lambda_{\min}}{\lambda_{\max} - \lambda_{\min}} \text{ or } \mu = \frac{-\lambda_{\min}}{1 - \lambda_{\min}}$$

$$\text{VAR}(Y) = \frac{\mathbf{1}^T \mathbf{C} \mathbf{1}}{n(\lambda_{\max} - \lambda_{\min})^2} \text{ or } \frac{\mathbf{1}^T \mathbf{D}^{-1} \mathbf{C} \mathbf{D}^{-1} \mathbf{1}}{n(1 - \lambda_{\min})^2},$$

where \mathbf{D} is a diagonal matrix whose (i, i) element is $1/\sum_{j=1}^n C_{ij}$. Furthermore, the moments of the distribution of eigenvalues are easy to calculate. The first moment, or mean, is zero, by definition. In addition, the second, third, and fourth moments can be determined exactly for a given K_4 , and in the limit as $K_4 \rightarrow \infty$:

$$\text{Variance} = \frac{82K_4 + 13}{288K_4}, K_4 > 1; \lim_{K_4 \rightarrow \infty} \frac{82K_4 + 13}{288K_4} = \boxed{\frac{41}{144}}$$

$$m'_3 = \frac{21K_4 + 10}{144K_4}, K_4 > 1; \lim_{K_4 \rightarrow \infty} \frac{21K_4 + 10}{144K_4} = \boxed{\frac{7}{48}}$$

$$m'_4 = \frac{7462K_4 + 2869}{41472K_4}, K_4 > 1; \lim_{K_4 \rightarrow \infty} \frac{7462K_4 + 2869}{41472K_4} = \boxed{\frac{2869}{41472}}.$$

A nonlinear regression analysis of selected K_4 empirical moments confirm these results.

Furthermore, the sum of positive eigenvalues and their squares can be approximated using nonlinear regression estimation, both of which have $R^2 \approx 1$, yielding

$$\frac{\sum_{i=1}^n \lambda_i^+}{n} = 0.22255 + \frac{0.02660}{K_4} \quad \text{and} \quad \frac{\sum_{i=1}^n (\lambda_i^+)^2}{n} = 0.19980 + \frac{0.04690}{K_4}.$$

These equations allow estimation of the parameters of the following two nonlinear regression equations:

$$\hat{\lambda} = \frac{j-1}{n-1} e^{b_n} e^{-b_n \frac{j-1}{n-1}}; \hat{\lambda} < 0 \quad \text{and} \quad \hat{\lambda} = \frac{n-j}{n-1} e^{b_p} e^{-b_p \frac{n-j}{n-1}}; \hat{\lambda} > 0,$$

Table 1

Output statistics for the eigenvalue distribution of single linked K_4 chain graphs with λ and $\hat{\lambda}$

	Mean	Std. Dev.	Minimum	Maximum	Skewness	Kurtosis
λ	-5.44981×10^{-16}	0.5341391	-0.4999949	1.0	0.9628461	-0.7771001
$\hat{\lambda}$	-0.000213052	0.5342607	-0.4999949	1.0	0.9869029	-0.7766108

where p denotes the percentage of n^- , with estimated values $b_n = 1$ and $b_p = 0.5909$. These equations have a combined $R^2 = 0.9989$, and summary statistics as displayed in Table 1. Figure 2 portrays example output of these summary statistics.

Likewise, Figures 2–3 demonstrate a Jacobian approximation for this example, where p is 0.75 and the exact and approximated Jacobian values are represented by the following equation:

$$J = \left(\frac{\rho}{2n}\right) (J_{a2} \lambda_{min}^2 - J_{a1} \lambda_{max}^2) + \left(\frac{1}{n}\right) \left[(J_{a2} |\lambda_{min}|) \log\left(\frac{J_{d2}}{|\lambda_{min}|}\right) + J_{a1} \lambda_{max} \log\left(\frac{J_{d1}}{\lambda_{max}}\right) - J_{a2} |\lambda_{min}| \log\left(\frac{J_{d2}}{|\lambda_{min}|} + \rho\right) - J_{a1} \lambda_{max} \log\left(\frac{J_{d1}}{\lambda_{max}} - \rho\right) \right]$$

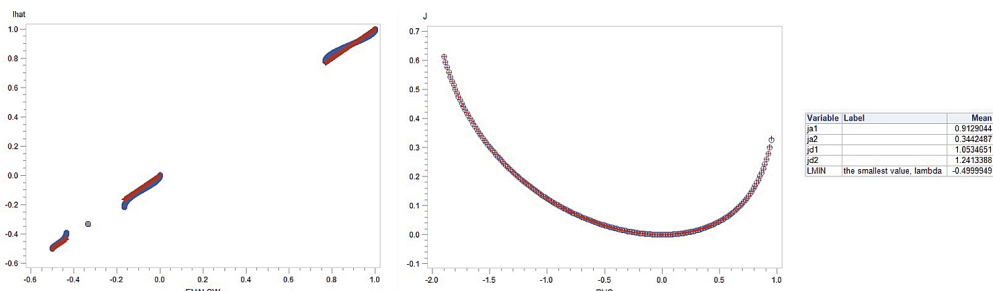


Fig. 2. Left: example output associated with Table 1; Center and Right: The exact results of the Jacobian term for $p = 0.75$

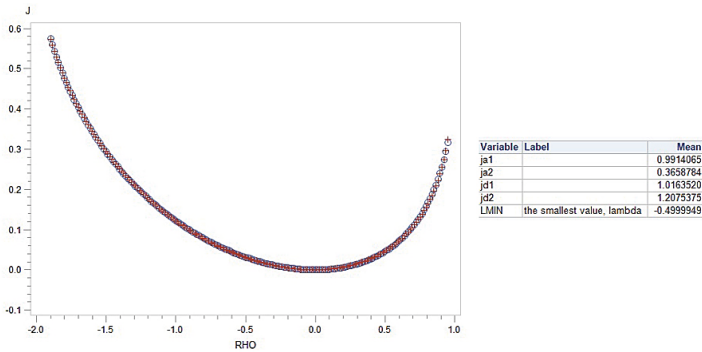


Fig. 3. The approximated results of the Jacobian term for $p = 0.75$

To analyze specification error, we approximate the Jacobian based upon the estimated eigenvalues. We do this for percentages of 0.75, 2/3, and 0.60. Figure 4 portrays these graphs.

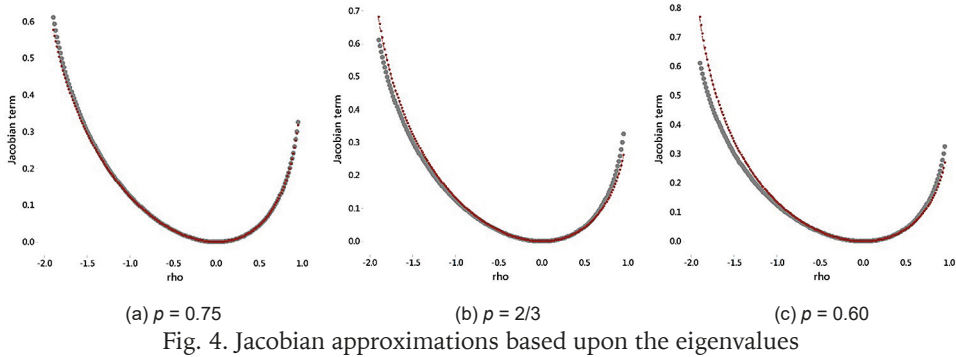


Fig. 4. Jacobian approximations based upon the eigenvalues

Table 2 reports estimation bias from the Jacobian specification error, assuming the stated percentage of negative eigenvalues for 200 K_4 subgraphs and 1,000 simulation replications.

Table 2

Estimation bias from Jacobian specification error: $K_4 = 200$; 1,000 replications

	exact ($r = 100$)	75%	67%	t75%-67%	60%	t75%-60%
0.9	0.898 (0.009)	0.898 (0.008)	0.921 (0.008)	-985.1	0.917 (0.008)	-918.9
0.5	0.499 (0.029)	0.500 (0.030)	0.513 (0.031)	-350.1	0.512 (0.031)	-385.2
0.0	-0.013 (0.048)	-0.010 (0.047)	-0.007 (0.047)	-451.3	-0.006 (0.046)	-336.0
-0.5	-0.507 (0.055)	-0.509 (0.052)	-0.493 (0.050)	-281.2	-0.487 (0.049)	-213.0
-0.9	-0.901 (0.048)	-0.908 (0.052)	-0.871 (0.049)	-361.6	-0.854 (0.047)	-333.9
-1.5	-1.499 (0.034)	-1.522 (0.035)	-1.452 (0.034)	-1251.3	-1.409 (0.033)	-1121.7

2. Initial Results

Our analysis begins with a general examination of connected planar graphs. Then, we examine specific specimen sets of such graphs, all of which contain at least one K_4 subgraph. These results establish part of the foundation for our work.

2.1. An Initial Review of Planar Graphs

Our analysis treats several different types of graphs, focusing only on connected planar graphs such as those illustrated in *An Atlas of Graphs* [2005]. This book enumerates all of the graphs containing one to seven vertices. The total number of graphs illustrated in its pertinent section is 1,252, although we examined substantially fewer graphs because we restricted our attention to the class of connected graphs. This book also presents graphs that are *not* connected.

Our results reveal that of the 261 connected planar graphs that are studied, only 104 contain K_4 subgraphs. Of those, only two graphs contain a proportion n^-/n greater than $\frac{2}{3}$ (the conjectured bound of Griffith and Luhanga [2011]). The configurations of these two graphs are: (1) the K_4 subgraph, and, (2) a graph containing two K_4 subgraphs sharing a single node. Figure 5 portrays a modification of this latter graph.

We focus on these two particular graphs to identify specimen sets of graphs for further analysis. We subsequently describe the other configurations of our focus. The purpose of studying these specimens is three-fold: (1) to determine if these or other similar configurations converge to $\frac{2}{3}n$ as the number of K_4 subgraphs increases; (2) to extract other sets of K_4 subgraphs for further examination; and, (3) to determine whether or not increasing the number of K_4 subgraphs results in an asymptotically decreasing value of n^-/n .

2.2. Specimen Sets of Planar Graphs

The graph specimen that we are most interested in is the one yielding the original counterexample to [6] – the K_4 complete planar graph. As noted previously, our focus includes the set of graphs comprising K_4 subgraphs sharing a single node. For this configuration, as the number of K_4 subgraphs increases, $\frac{n^-}{n}$ appears to converge to $\frac{2}{3}$. Figure 5 illustrates this specimen graph, and Figure 13 portrays its convergence trajectory.

Figure 13 motivates an inspection of other specimens that are similar in construction, in that they contain many K_4 subgraphs that are connected in various consistent ways. Figure 6 illustrates one such example, another patterned specimen graph constructed with K_4 subgraphs. These graphs are the collection of K_4 subgraphs sharing

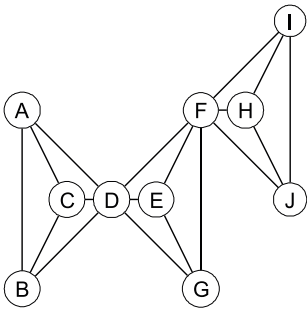
a single node. Our results again show that the percentage of negative eigenvalues converges to $\frac{2}{3}$ as $n \rightarrow \infty$. Figure 13 portrays this implied convergence.

Four variations of Figure 6 are of interest. Figure 7 illustrates the first variation, which depicts K_4 subgraphs connected to a shared node by individual edges. The second variation consists of K_4 subgraphs connected to their neighbors by edges such that the center of the graph becomes increasingly circular. Figure 8¹ illustrates this specimen set of graphs. Figure 9 illustrates the third variation, a combination of the last two, where the center of the graph resembles a “wheel” containing a central node and K_4 neighbors connected by edges like wheel spokes. Figure 10 portrays the fourth variation, which is similar to Figure 8, but with the exception that the K_4 subgraphs are connected by their bottom nodes. Although the results of these four specimens differ slightly, in general, as the number of K_4 subgraphs increases, the total number of n^- for all four specimens converges to $\frac{3}{4}n$, as illustrated in Figures 13 and 16.

In addition to the aforementioned specimen graph configurations, other examples of specimen graphs containing K_4 subgraphs exist, one of which is illustrated in Figure 8. In this example, a series of K_4 subgraphs has neighbors connected by two edges, where each edge connects a different pair of nodes. Figure 10 portrays an example of these graphs. Our analysis shows that the percentage of negative eigenvalues for this specimen category of graphs eventually converges to $\frac{2}{3}$, as illustrated in Figure 15.

Table 3

Specimen graphs resembling “wheel-like” configurations

Specimen Graph	Graph Generation Description
 <p style="text-align: center;">Figure 5</p>	<p>Snake configuration</p> <p>The second graph containing a $n^- \leq \frac{2}{3}n$ in <i>An Atlas of Graphs</i>, cataloged as G1009.</p> <p>Generation of this specimen graph involves adding another K_4 sub-graph directly to the left-most or right-most node of the current graph configuration.</p> <p>Note that this graph can be re-drawn to resemble a variation of the wheel configuration (Fig. 8)</p>

¹ The regression analysis for this specimen set of graphs excluded the first two data points. These points are outliers whose exclusion simplifies approximation of the general trend.

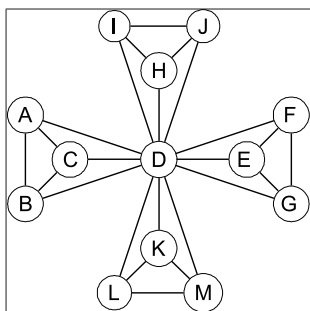


Figure 6

Pinwheel configuration

Graphs containing K_4 subgraphs connected by a central node. Generation of this specimen graph involves increasing K_4 subgraphs around a central node. This central node is one of the four nodes constituting each K_4 subgraph

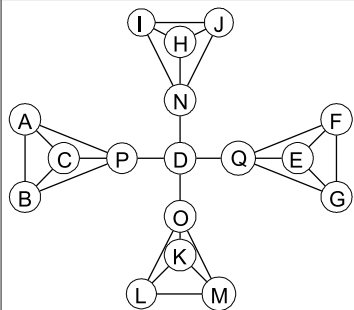


Figure 7

Extended pinwheel configuration

Graphs containing K_4 subgraphs connected to a central node by individual edges. Note that each K_4 subgraph is connected to a central node by a single edge. Neither the connecting edge nor the central node are part of the K_4 subgraphs

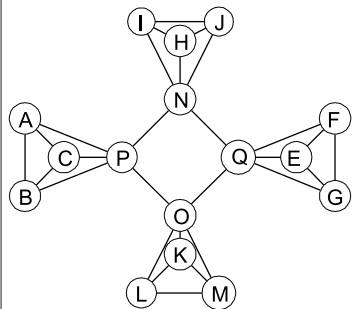


Figure 8

Wheel configuration

K_4 subgraphs connected by edges forming an interior wheel. Note the absence of an interior node, and that the connecting edges are generated from the same node within each K_4 subgraph

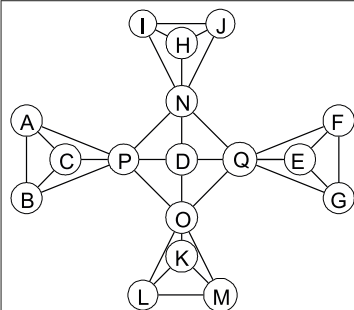


Figure 9

Wagon wheel configuration

A graph containing K_4 subgraphs whose center resembles a "wagon wheel". Note the presence of a central node connected by one edge from each K_4 subgraph *as well as* edges connecting each K_4 subgraph by a K_4 node. This configuration is a combination of the extended pinwheel and wheel configurations (Fig. 6, 8)

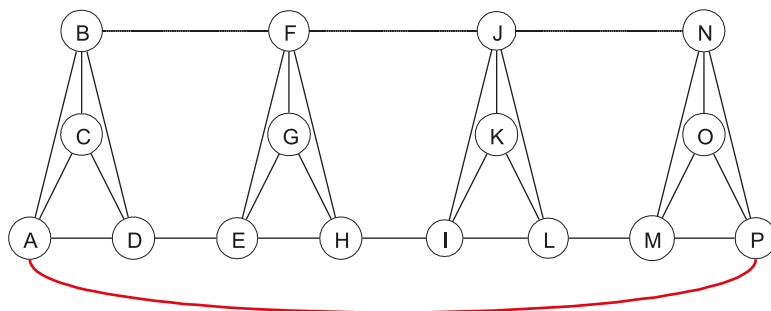


Fig. 10. Three variations of single-linked K_4 subgraphs. The **first variation** contains only solid black edges and consists of single linked K_4 subgraphs. The **second variation** comprises both solid and dashed black edges, making up K_4 subgraphs connected by two links. The **third variation** involves both solid black and **solid red** edges

Employing individual specimen graphs, we can begin building tessellations of K_4 subgraphs. The first considered here is a $p \times q$ tessellation of squares constructed with K_4 subgraphs. Figure 11a illustrates these types of graphs. Expanding this square tessellation from two K_4 subgraphs (i.e., a single square or a 1×1 tessellation) through a 2,000 K_4 subgraph tessellation, the percentage of negative eigenvalues converges to 0.50, as illustrated in Figure 11b. This is the maximum percentage for a regular square tessellation coupled with a rook's adjacency rule.

The final specimen graphs examined consist of K_4 subgraphs arranged as hexagons around a center node, as illustrated in Figure 12a. More importantly, these hexagons are arranged in a $p \times q$ tessellation, where p is the number of hexagons in

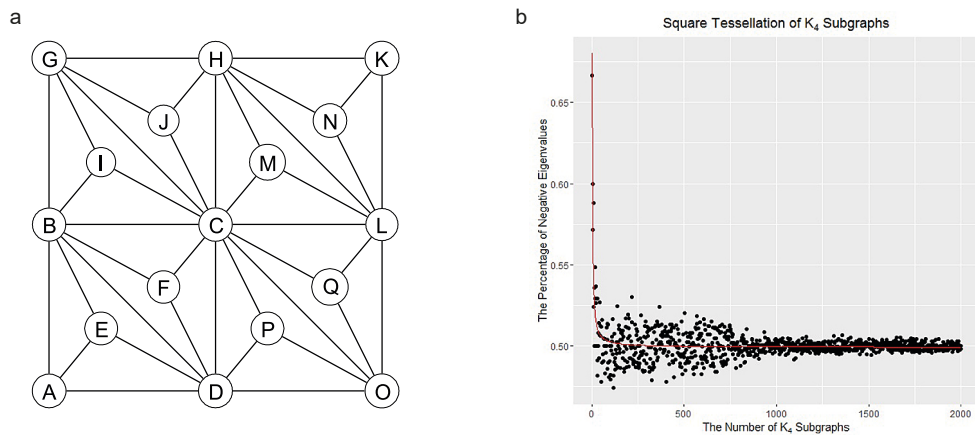


Fig. 11. Square tessellations of K_4 subgraphs have a percentage of n^- that converges to 0.50. Note that values where $p=q$ in the tessellation dimension have a tighter fit along the regression line

- (a) An example of a 2×2 square tessellation, (b) A square tessellation of K_4 subgraphs comprising K_4 subgraphs. As the $p \times q$ dimension expands, $\frac{n^-}{n}$ converges to 0.50.

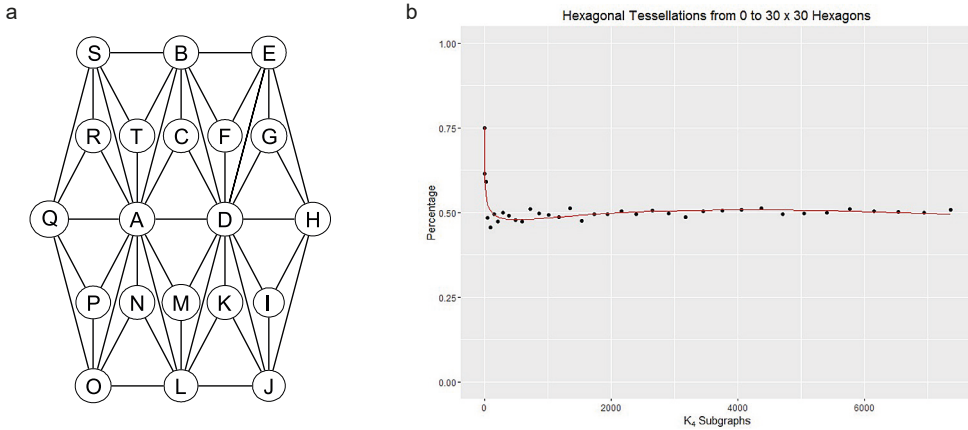


Fig. 12. Hexagonal tessellations of K_4 subgraphs have a percentage of n^- that converges to 0.50. Note that observations plotted are tessellations for which $p=q$

(a) A hexagonal tessellation of K_4 subgraphs, (b) Hexagonal tessellation results from $p,q=0$, (i.e., only a single K_4) to $p,q=30$.

the horizontal axis, and q is the number of hexagons in the vertical axis. For $p,q=0$ (i.e., $K_4=1$), the percentage of n^- is 0.75, as previously discussed. As p and q increase, the percentage of n^- decreases, eventually converging to approximately 0.50, as illustrated in Figure 12b.

Evidence summarized here supports our initial conjecture about the convergence of the percentage of negative eigenvalues. However, graphs exist for which K_4 subgraphs result in the percentage of negative eigenvalues remaining consistently at $\frac{3}{4}$. That being said, we can state the following, as Theorem 1 and Conjecture 1.

Theorem 1. The existence of K_4 subgraphs in a connected planar graph is a necessary, but not a sufficient, condition for the percentage of n^- to be $\frac{3}{4}$.

Proof.

Figure 5, where the specimen set of planar graphs contains K_4 subgraphs sharing a single node, illustrates one of several counterexamples corroborating Theorem 1. As the number of K_4 subgraphs increases, the percentage of n^- converges to $\frac{2}{3}$, as illustrated in Figure 13.

Conjecture 1. For connected planar graph spectra based on n nodes whose articulation **does not** contain K_4 subgraphs, the maximum n^- is bounded by

$$n^- \leq \frac{2}{3}n. \quad (4)$$

An additional example we study is a series of K_4 subgraphs with neighbors that are connected by one edge, as illustrated by Figure 10. Expanding this general graph implies that the percentage of n^- always is $\frac{3}{4}n$ for it. This finding shows that more

than a single set of graphs exist whose percentage of negative eigenvalues exceeds the $\frac{2}{3}$ conjecture, rather than asymptotically decreasing to $\frac{2}{3}$. Figure 14 illustrates this contention.

3. Single Linked K_4 Chains

The following are two theorems that give the maximum number of -1 eigenvalues for special K_4 chains connected by single links. *The Appendices present proofs of these theorems.*

Theorem 2. The number of -1 eigenvalues for the K_4 chain (Fig. 14) is $\tau+2$, where τ denotes the number of K_4 subgraphs.

Table 4

Convergence trajectory plots for percentages of negative eigenvalues

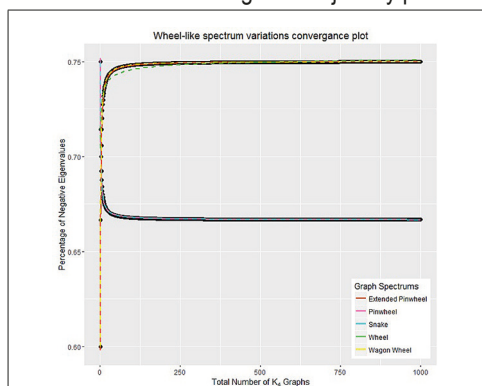


Fig. 13. Plots associated with the aforementioned “wheel-like” graphs, as illustrated in Table 3

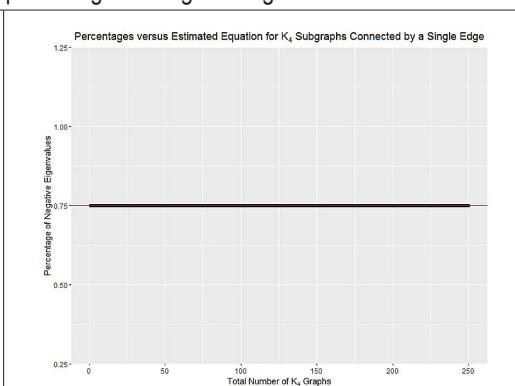


Fig. 14. Results for Figure 10 – implied convergence for a chain of K_4 subgraphs with neighbors connected by single edges

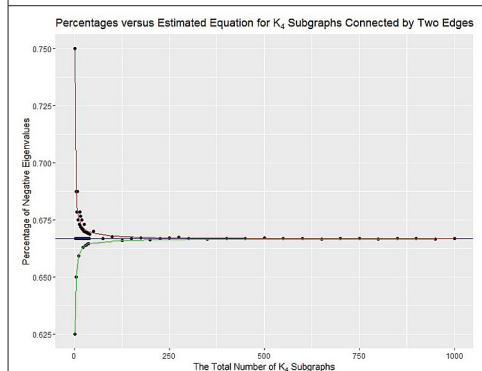


Fig. 15. Results for Figure 10 – implied convergence for a chain of K_4 subgraphs with neighbors connected by two edges

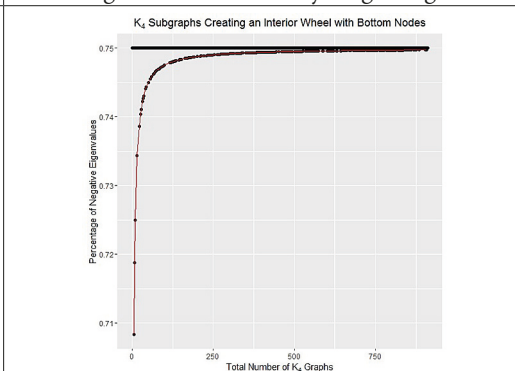


Fig. 16. Results for Figure 10 – implied convergence for a chain of K_4 subgraphs with neighbors connected by two bottom nodes and forming a closed circle

Theorem 3. The number of -1 eigenvalues for K_4 subgraphs directly connected by nodes can be calculated with

$$\sum \lambda_{-1} = \begin{cases} 3, & \tau > 1 \\ 2\tau, & \tau = 1 \end{cases},$$

where τ denotes the number of K_4 subgraphs.

4. Simulation Experiments

Planar graphs can be generated in a number of ways (e.g., see Meinert, Wagner [2011]). A new algorithm exploiting the mixture of a regular square and hexagonal tessellation structure generated the simulation experiment results this section summarizes. It is capable of producing the full range of connected planar graphs: a linear, regular square or hexagonal, maximum connectivity, or irregular surface partitioning. Although it yields graphs whose sizes range from 2 to 4,489, because of the random sampling involved, the central tendency for graph size is a mean of 1,156, a median of 870, and a mode of 120; its frequency distribution resembles that for a gamma random variable. This algorithm also allows replicates for a specified n , and a shift in its emphasis between the regular square and hexagonal tessellations. Not only do numerous isomorphisms and automorphisms of randomly selected planar graphs exist, but an enormous number of different graphs exist for most n .

A database of 184 specimen empirical surface partitionings furnish a yardstick for comparisons. Figure 17a portrays the principal eigenvalues histogram for the binary 0–1 adjacency matrices depicting the dual graphs of these selected surfaces (n is between 5 and 7,249); its range is 2.94 to 8.60. Figure 17b portrays the principal eigenvalues histogram for 10,000 randomly generated planar graphs (n is between 3 and 4,292); its range is 1.41 to 15.06. This range is wider because observing maximum connectivity planar graphs is uncommon in practice, and geographic landscapes partitioned into too few areal units rarely are analyzed.

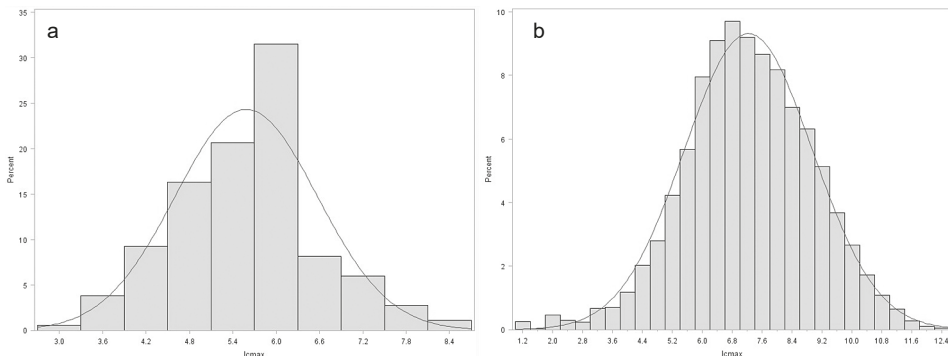


Fig. 17. Histograms of principal eigenvalues of the binary spatial weights matrix C
 (a) For 184 specimen surface partitions, (b) For 10,000 randomly generated planar graphs.

The variable of interest here is the percentage of n^- . Figure 18 portrays the inertia components of the randomly generated planar graphs. For reasonable size n , the maximum percentage is 65, below the $\frac{2}{3}$ threshold. Figure 18b portrays a scatterplot of the predicted and observed values for $n \geq 6$ (removing this constraint introduces a few anomalies, and only marginally decreases the percentage of variance accounted for); its pseudo- R^2 is 0.92.

The trend line is described as follows: $\% i = \frac{1}{1+e^{-a_i}}$, where $a_i = -2.2392 - 0.0158 \lambda_{c \max_i} + 0.203 \lambda_{w \min_i} + 0.0742 \text{VAR}_{c_i} + 2.3023 \text{VAR}_{w_i}$, with $\lambda_{c \max_i}$ denoting the principal eigenvalue of the binary 0–1 spatial weights matrix \mathbf{C} , $\lambda_{w \min_i}$ denoting the minimum eigenvalue of the row-standardized spatial weights matrix \mathbf{W} , VAR_{c_i} denoting the variance of the eigenvalues of matrix \mathbf{C} , and VAR_{w_i} denoting the variance of the eigenvalues of matrix \mathbf{W} . All of these quantities are available for a given spatial weights matrix.

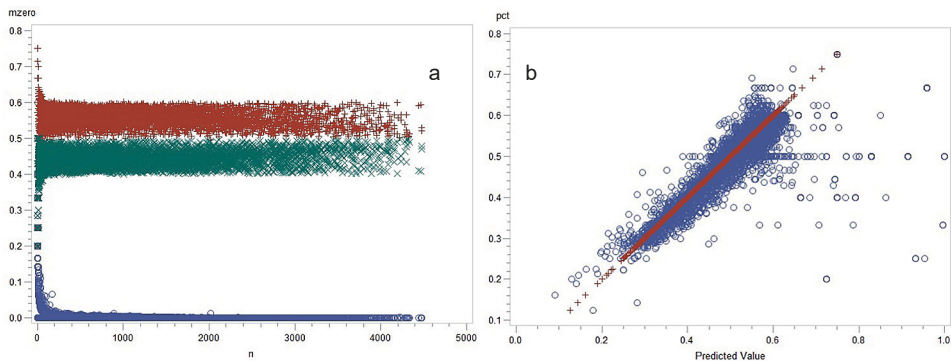
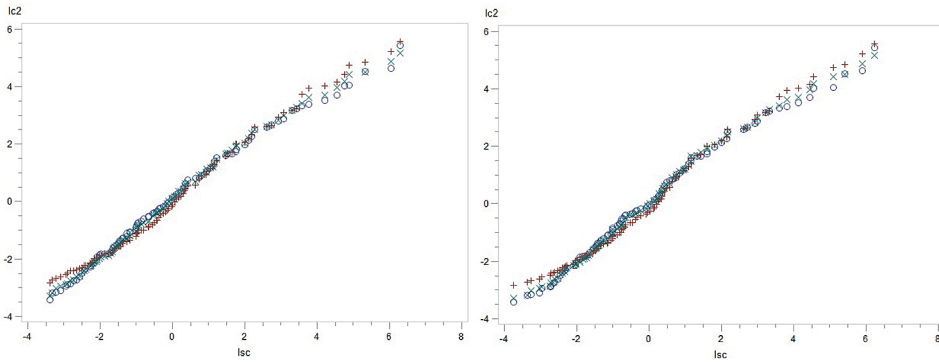


Fig. 18. (a) The inertia components of a binary 0–1 spatial weights matrix \mathbf{C} : red denotes % negative, green denotes % positive, and blue denotes % zero eigenvalues. (b) A scatterplot with a superimposed binomial regression model prediction of the percentage of negative eigenvalues

Conjecture 2. Eigenvalues ranked (in descending order) $2k$ through $3k+1$ are -1 for matrix \mathbf{C} , and $-\frac{1}{3}$ for matrix \mathbf{W} .

Comparing the structure of the empirical specimens and selected random planar graphs reveals similarities and differences. Figure 19 (after Garcia [2012]) portrays two extreme cases in a set of seven, for $n=99$; this scatterplot is similar to a quantile plot, with a straight line depicting a close correspondence. This figure illustrates that some of the simulated graphs are similar to empirical graphs, and others are not. Figure 19a is for a graph with a principal eigenvalue of 6.40, whereas Figure 19b is for a graph with a principal eigenvalue of 8.94; principal eigenvalues for the three specimen surfaces range from 5.18 to 5.55.

In conclusion, the simulation experiments support the contention that most percentages of negative eigenvalues are less than $\frac{2}{3}$ and suggest that for practical values of n , this percentage may well be between 50% and 60%.



(a) A close correspondence

(b) A poor correspondence

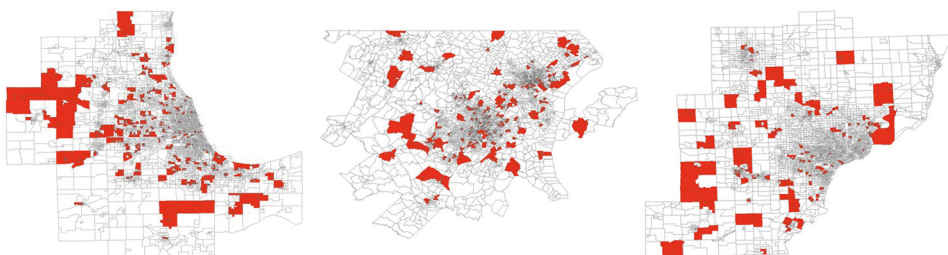
Fig. 19. Three empirical specimen sets of eigenvalues superimposed on those for a simulated random graph (denoted by open circles); $n = 99$

4.1. K_4 Subgraphs and Empirical Surface Partitionings

Complimentary to the simulation experiments described in the previous section is an analysis of K_4 subgraphs in empirical surface partitionings. Here these surface partitionings consist of major cities of North America, including: Chicago, Washington, Detroit, and Philadelphia.

In all cases, more K_4 subgraphs are present than was first anticipated. Despite the presence of these surprisingly large numbers of K_4 subgraphs, our overall results in terms of negative eigenvalue percentages do not change.

One possible explanation for several clusters of K_4 subgraphs in cities lies in large and irregular administrative polygon (e.g., census tract) sizes, which often comprise oblong water bodies, such as rivers. These boundaries connect to several other boundaries in a way that generates K_4 subgraphs as well as the clustering of K_4 subgraphs, similar to that appearing in Figure 6. An example of this phenomena is illustrated in Figures 21a–21b.



(a) Chicago, Illinois

(b) Washington, DC

(c) Detroit, Michigan

Fig. 20. The presence of K_4 subgraphs in the Chicago, Washington, and Detroit MSAs



(a) Philadelphia, Pennsylvania (b) A zoom-in of Philadelphia
 Fig. 21. The presence of K_4 subgraphs in the Philadelphia MSA

4.1.1. n^- and Empirical Surface Partitionings

A further examination of empirical surface partitionings for several metropolitan statistical areas (MSAs) in the United States suggests that the percentage of negative eigenvalues remains well below the $\frac{2}{3}$ threshold. For several MSAs studied, n^- remains below 0.60. Note that data utilized here are from the 2016 census tracts from the TIGER/Line website (<https://www.census.gov/cgi-bin/geo/shapefiles/index.php>).

Calculating the rook adjacency spatial weights matrices for twenty MSAs, ranging in size from small to large in terms of number of census tracts, reveals that the highest percentage of n^- is 0.632, with a mean percentage of 0.586. Table 5 tabulates summary results for the selected MSAs. Overall, these results support our hypothesis that the utilized maximum bound for the percentage of n^- should be significantly less

than $\frac{3}{4}$.

4.1.2. K_4 Subgraphs in Empirical Surface Partitionings

In addition to examining n^- in the preceding section, we also examine the number of K_4 subgraphs in empirical surface partitionings. Several sizes of MSAs were analyzed, as detailed in Table 5.

As illustrated in Figure 22, the spread of n^- is fairly consistent regardless of the percentage of census tracts contributing to K_4 subgraphs. In addition, all examples— with the exception of the Bloomsberg-Berwick, Pennsylvania MSA (a small-scale MSA in the United States) – have a percentage of census tracts in K_4 subgraphs well under 25%. Specifically, 50% of our sampled MSAs have less than 10% of their census tracts contributing to K_4 subgraphs, with 75% of our sampled MSAs having under 15%.

Table 5

United States MSA Census Tract Based K_4 and n^- Results

MSA	# Census Tracts	# K_4 s	n^-/n
Bloomsburg-Berwick, PA	19	3	0.632
New York-Newark-Jersey City, NY-NJ-PA	4,700	138	0.584
Corvallis, OR	18	0	0.556
Elmira, NY	22	1	0.591
Grand Island, NE	22	0	0.591
Parkersburg-Vienna, WV	28	0	0.607
Deltona-Daytona Beach-Ormond Beach, FL	135	3	0.585
Des Moines-West Des Moines, IA	131	7	0.580
Madison, WI	133	7	0.579
Ogden-Clearfield, UT	117	6	0.607
Springfield, MA	139	5	0.583
Syracuse, NY	186	9	0.581
Wichita, KS	152	8	0.592
Winston-Salem, NC	150	3	0.580
Boston-Cambridge-Newton, MA-NH	1,006	29	0.589
Chicago-Naperville-Elgin, IL-IN-WI	2,215	45	0.574
Dallas-Fort Worth-Arlington, TX	1,324	42	0.582
Houston-The Woodlands-Sugar Land, TX	1,072	27	0.576
Los Angeles-Long Beach-Anaheim, CA	2,928	45	0.580
Philadelphia-Camden-Wilmington, PA-NJ-DE-MD	1,477	68	0.587

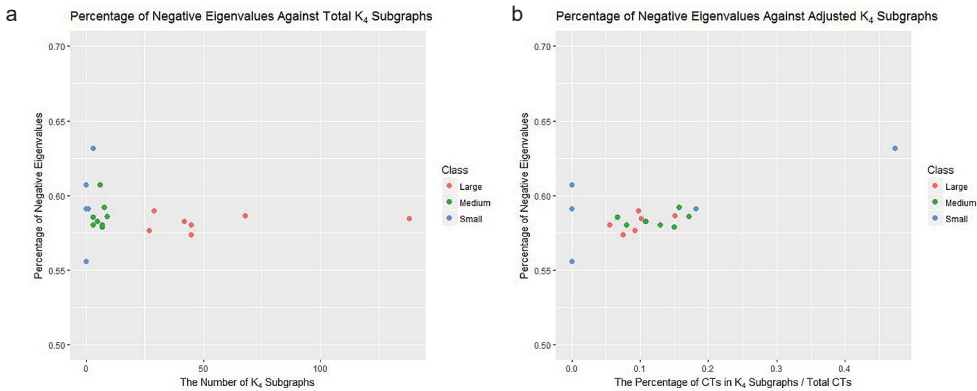


Fig. 22. (a) A scatterplot of the percentage of n^- versus the number of K_4 s, (b) A scatterplot of the percentage of n^- versus the percentage of census tracts in K_4 s

5. Further Work

Although more work remains to be done, our current findings yield promising results that make us confident that our goals set out in this paper will be accomplished in the near future. A proof of Conjecture 1 is anticipated. That being said, we must emphasize that construction of such a formal proof is challenging.

Now that we have seen instances for which specimen graphs containing K_4 subgraphs stay consistently above our conjectured bound, we are interested in determining the implications of these instances, and seeing what happens as our specimen set expands in size.

Nevertheless, the ultimate goal of this work is to enable a sound Jacobian term estimate via approximated eigenvalues for massively large georeferenced datasets, one comparable to that furnished by Griffith [2015] for remote sensing datasets.

References

- Bivand R., Hauke J., Kossowski T., 2013, *Computing the Jacobian in Gaussian spatial autoregressive models: An illustrated comparison of available methods*, *Geographical Analysis*, 45(2): 150–179.
- Boots B., Royale G., 1991, *A conjecture on the maximum value of the principal eigenvalue of a planar graph*, *Geographical Analysis*, 23(3): 276–282.
- Elphick C., Wocjan P., 2016, *An inertial lower bound for the chromatic number of a graph*, arXiv, 1–7.
- Garcia C., 2012, *A simple procedure for the comparison of covariance matrices*, *BMC Evolutionary Biology*, 12, 222.
- Griffith D.A., 2015, *Approximation of Gaussian spatial autoregressive models for massive regular square tessellation data*, *International Journal of Geographical Information Science*, 29(12): 2143–2173.
- Griffith D.A., Luhanga U., 2011, *Approximating the inertia of the adjacency matrix of a connected planar graph that is the dual of a geographic surface partitioning*, *Geographical Analysis*, 43: 383–402.
- Meinert S., Wagner D., 2011, *An experimental study on generating planar graphs*, *Karlsruhe Reports in Informatics*, 13.
- Read R., Wilson R., 2005, *An atlas of graphs*, Oxford University Press, New York.
- Tait M., Tobin J., 2016, *Three conjectures in extremal spectral graph theory*, arXiv, 1–26.

Appendices: proofs of theorems

A. -1 eigenvalues for K_4 subgraph chains

Theorem 2. The number of -1 eigenvalues for the K_4 chain is $\tau+2$, where τ denotes the number of K_4 subgraphs.

Proof.

By induction. Note that the following argument is presented for the \mathbf{C} matrix; however, the same process holds for the \mathbf{W} matrix. In the latter case, the eigenvalues isolated are $-\frac{1}{3}$ rather than -1 .

Let $\tau=1$. Then, for one K_4 subgraph, to calculate the number of -1 eigenvalues, one can create the adjusted K_4 subgraph matrix with $-\lambda$ multiplied by the identity matrix, such that $K_4 - \lambda I$. This adjustment leads to the eigenvalue problem, where $\det|K_4 - \lambda I| = 0$, and

$$K_4 - \lambda I = \begin{bmatrix} -\lambda & 1 & 1 & 1 \\ 1 & -\lambda & 1 & 1 \\ 1 & 1 & -\lambda & 1 \\ 1 & 1 & 1 & -\lambda \end{bmatrix}.$$

To determine the number of eigenvalues of value -1 , which can be represented as $-(\lambda+1)$, using matrix theory, one can isolate these values in single columns such that only the $-(\lambda+1)$ terms and zeros are present. From there, one can simply solve for λ in each column. For the following matrix algebra displayed in this document, let C_i and R_i represent the i^{th} column and row of the matrix, respectively. Beginning with the $K_4 - \lambda I$ matrix, we perform the following matrix algebra operations to isolate as many $-(\lambda+1)$ as possible:

$$\begin{bmatrix} -\lambda & 1 & 1 & 1 \\ 1 & -\lambda & 1 & 1 \\ 1 & 1 & -\lambda & 1 \\ 1 & 1 & 1 & -\lambda \end{bmatrix} \xrightarrow{C_1 - C_2 = C_1} \begin{bmatrix} -\lambda - 1 & 1 & 1 & 1 \\ \lambda + 1 & -\lambda & 1 & 1 \\ 0 & 1 & -\lambda & 1 \\ 0 & 1 & 1 & -\lambda \end{bmatrix}$$

$$\begin{bmatrix} -\lambda - 1 & 1 & 1 & 1 \\ \lambda + 1 & -\lambda & 1 & 1 \\ 0 & 1 & -\lambda & 1 \\ 0 & 1 & 1 & -\lambda \end{bmatrix} \xrightarrow{R_2 - R_1 = R_2} \begin{bmatrix} -\lambda - 1 & 1 & 1 & 1 \\ 0 & -\lambda + 1 & 2 & 2 \\ 0 & 1 & -\lambda & 1 \\ 0 & 1 & 1 & -\lambda \end{bmatrix}$$

Continuing with this process, we can isolate other values of $-(\lambda+1)$.

$$\begin{bmatrix} -\lambda - 1 & 1 & 1 & 1 \\ 0 & -\lambda + 1 & 2 & 2 \\ 0 & 1 & -\lambda & 1 \\ 0 & 1 & 1 & -\lambda \end{bmatrix} \xrightarrow{\begin{matrix} C_2 - C_3 = C_2 \\ R_2 + R_3 = R_3 \end{matrix}} \begin{bmatrix} -\lambda - 1 & 0 & 1 & 1 \\ 0 & -\lambda - 1 & 2 & 2 \\ 0 & 0 & 2 - \lambda & 3 \\ 0 & 0 & 1 & -\lambda \end{bmatrix}$$

$$\begin{bmatrix} -\lambda - 1 & 0 & 1 & 1 \\ 0 & -\lambda - 1 & 2 & 2 \\ 0 & 0 & 2 - \lambda & 3 \\ 0 & 0 & 1 & -\lambda \end{bmatrix} C_3 - C_4 = C_3 \xrightarrow{R_3+R_4=R_4} \begin{bmatrix} -\lambda - 1 & 0 & 0 & 1 \\ 0 & -\lambda - 1 & 0 & 2 \\ 0 & 0 & -\lambda - 1 & 3 \\ 0 & 0 & 0 & 3 - \lambda \end{bmatrix}$$

Therefore, we can conclude that for $\tau=1$, the number of -1 eigenvalues is equal to 3. For $\tau = 2$, we continue to utilize the same process, but now the $\tau=1$ and the $\tau=2$ parts of the matrix can have only two $\lambda = -1$ values isolated, as illustrated next:

$$\begin{bmatrix} -\lambda & 1 & 1 & 1 & 0 & 0 & 0 & 0 \\ 1 & -\lambda & 1 & 1 & 0 & 0 & 0 & 0 \\ 1 & 1 & -\lambda & 1 & 0 & 0 & 0 & 0 \\ 1 & 1 & 1 & -\lambda & 1 & 0 & 0 & 0 \\ 0 & 0 & 0 & 1 & -\lambda & 1 & 1 & 1 \\ 0 & 0 & 0 & 0 & 1 & -\lambda & 1 & 1 \\ 0 & 0 & 0 & 0 & 1 & 1 & -\lambda & 1 \\ 0 & 0 & 0 & 0 & 1 & 1 & 1 & -\lambda \end{bmatrix} \rightarrow \begin{bmatrix} -\lambda - 1 & 0 & 1 & 1 & 0 & 0 & 0 & 0 \\ 0 & -\lambda - 1 & 2 & 2 & 0 & 0 & 0 & 0 \\ 0 & 0 & -\lambda - 2 & 3 & 0 & 0 & 0 & 0 \\ 0 & 0 & 1 & -\lambda & 1 & 0 & 0 & 0 \\ 0 & 0 & 0 & 1 & -\lambda & 1 & 0 & 0 \\ 0 & 0 & 0 & 0 & 3 & -\lambda - 2 & 0 & 0 \\ 0 & 0 & 0 & 0 & 2 & 2 & -\lambda - 1 & 0 \\ 0 & 0 & 0 & 0 & 1 & 1 & 0 & -\lambda - 1 \end{bmatrix}$$

Thus, 4 isolated $(-1-\lambda)$ terms exist for $\tau=2$. This is due to the cell entries of 1 directly below and to the right of the λ in column 4. These cell values connect the two K_4 subgraphs and prevent the isolation of λ terms in columns 3, 4, 5, and 6.

If we continue to expand this matrix for $\tau=3$, the same process holds. Therefore, we can isolate 4 instances of $(-1-\lambda)$ terms:

$$\begin{bmatrix} -\lambda & 1 & 1 & 1 & 0 & 0 & 0 & 0 & 0 & 0 & 0 & 0 \\ 1 & -\lambda & 1 & 1 & 0 & 0 & 0 & 0 & 0 & 0 & 0 & 0 \\ 1 & 1 & -\lambda & 1 & 0 & 0 & 0 & 0 & 0 & 0 & 0 & 0 \\ 1 & 1 & 1 & -\lambda & 1 & 0 & 0 & 0 & 0 & 0 & 0 & 0 \\ 0 & 0 & 0 & 1 & -\lambda & 1 & 1 & 1 & 0 & 0 & 0 & 0 \\ 0 & 0 & 0 & 0 & 1 & -\lambda & 1 & 1 & 0 & 0 & 0 & 0 \\ 0 & 0 & 0 & 0 & 1 & 1 & -\lambda & 1 & 0 & 0 & 0 & 0 \\ 0 & 0 & 0 & 0 & 1 & 1 & 1 & -\lambda & 1 & 0 & 0 & 0 \\ 0 & 0 & 0 & 0 & 0 & 0 & 0 & 1 & -\lambda & 1 & 1 & 1 \\ 0 & 0 & 0 & 0 & 0 & 0 & 0 & 0 & 1 & -\lambda & 1 & 1 \\ 0 & 0 & 0 & 0 & 0 & 0 & 0 & 0 & 1 & 1 & -\lambda & 1 \\ 0 & 0 & 0 & 0 & 0 & 0 & 0 & 0 & 1 & 1 & 1 & -\lambda \end{bmatrix}$$

Without loss of generality,

$$\rightarrow \begin{bmatrix} -\lambda - 1 & 0 & 1 & 1 & 0 & 0 & 0 & 0 & 0 & 0 & 0 & 0 \\ 0 & -\lambda - 1 & 2 & 2 & 0 & 0 & 0 & 0 & 0 & 0 & 0 & 0 \\ 0 & 0 & -\lambda - 2 & 3 & 0 & 0 & 0 & 0 & 0 & 0 & 0 & 0 \\ 0 & 0 & 1 & -\lambda & 1 & 0 & 0 & 0 & 0 & 0 & 0 & 0 \\ 0 & 0 & 0 & 1 & -\lambda & 0 & 1 & 1 & 0 & 0 & 0 & 0 \\ 0 & 0 & 0 & 0 & 1 & -\lambda - 1 & 1 & 1 & 0 & 0 & 0 & 0 \\ 0 & 0 & 0 & 0 & 2 & 0 & -\lambda + 1 & 2 & 0 & 0 & 0 & 0 \\ 0 & 0 & 0 & 0 & 1 & 0 & 1 & -\lambda & 1 & 0 & 0 & 0 \\ 0 & 0 & 0 & 0 & 0 & 0 & 0 & 1 & -\lambda & 1 & 0 & 0 \\ 0 & 0 & 0 & 0 & 0 & 0 & 0 & 0 & 3 & -\lambda - 2 & 0 & 0 \\ 0 & 0 & 0 & 0 & 0 & 0 & 0 & 0 & 2 & 2 & -\lambda - 1 & 0 \\ 0 & 0 & 0 & 0 & 0 & 0 & 0 & 0 & 1 & 1 & 0 & -\lambda - 1 \end{bmatrix}$$

Now, when $\tau \geq 3$, every instance of τ that is *not* the first or last τ in the matrix is able to isolate 1 additional $(-1-\lambda)$ term. Therefore, we can assume that this is true for some arbitrary value of τ :

$$\begin{bmatrix} K_4(-\lambda I) & C & 0 & \cdots & \cdots \\ C^T & K_4(-\lambda I) & C & 0 & \cdots \\ 0 & C^T & \ddots & C & 0 \\ \vdots & 0 & C^T & \tau & 0 \\ \vdots & \cdots & 0 & 0 & \ddots \end{bmatrix},$$

where

$$C = \begin{bmatrix} 0 & 0 & 0 & 0 \\ 0 & 0 & 0 & 0 \\ 0 & 0 & 0 & 0 \\ 1 & 0 & 0 & 0 \end{bmatrix}.$$

and matrix C^T is the transpose of matrix C . The C and C^T components of the matrix exist due to the need to connect each K_4 subgraph. Therefore, there are $\tau-1$ instances of C and C^T when $\tau > 1$. These components of the matrix—namely the 1 element in C and C^T —prevent column-matrix algebra from isolating values of $\lambda = -1$ into either the column in which it is located, or into either the preceding or subsequent columns. The implication is that for any given matrix, we can isolate $\tau+2$ values of $\lambda = -1$ for any value of τ . The same process is relevant for $\tau+1$. The corresponding matrix for $\tau+1$ is

$$\begin{bmatrix} K_4(-\lambda I) & C & 0 & \cdots & \cdots \\ C^T & K_4(-\lambda I) & C & 0 & \cdots \\ 0 & C^T & \ddots & C & 0 \\ \vdots & 0 & C^T & \tau & C \\ \vdots & \cdots & 0 & C^T & \tau+1 \end{bmatrix}$$

From this preceding matrix for $\tau+1$, one can see by visual inspection that there are τ instances of the C and C^T components of the matrix.

Now we can compute the number of $\lambda = -1$. Based on our assertion, we should have $\tau+2$ instances of $\lambda = -1$. Because our $\tau = \tau+1$, then our adjusted value of $\lambda = -1$ is $\tau+3$. Because the first and last block of columns of $K_4(-\lambda I)$, C , and C^T yield 2 instances of $\lambda = -1$, we have $\tau-1$ K_4 subgraphs of the matrix remaining without any λ -values isolated. We know that each of the interior components of the full adjacency matrix yield another $\lambda = -1$, which gives us an additional $\tau-1$ instance of $\lambda = -1$. Summing these two values together, our adjusted number of occurrences for $\lambda = -1$ is $4 + (\tau-1) = \tau+3$. Thus, our assertion holds for all K_4 chain matrices.

B. -1 eigenvalues for K_4 subgraph connected by nodes

Theorem 3. The number of -1 eigenvalues for K_4 subgraphs directly connected by nodes can be calculated with,

$$\sum \lambda_{-1} = \begin{cases} 3, & \tau = 1 \\ 2\tau, & \tau > 1 \end{cases}$$

where τ denotes the number of K_4 subgraphs.

Proof.

By induction. Again, this argument utilizes the \mathbf{C} matrix; as for Appendix A, the same process holds for the \mathbf{W} matrix, with the isolated eigenvalues being $-\frac{1}{3}$ rather than -1 . The process is the same as the proof for Theorem 2. Again for $\tau=1$, the number of $-(\lambda+1)$ is 3.

In contrast with the Appendix A proof, we need to perform all columnar operations first, and then perform the row operations. We continue using the standard column and row symbols, C_i and R_i . For $\tau=2$, the column subtractions are as follows: $C_3 - C_2 = C_3$; $C_4 - C_2 = C_4$; $C_5 - C_7 = C_5$; $C_6 - C_7 = C_6$

$$\begin{bmatrix} -\lambda & 1 & 1 & 1 & 1 & 1 & 1 \\ 1 & -\lambda & 1 & 1 & 0 & 0 & 0 \\ 1 & 1 & -\lambda & 1 & 0 & 0 & 0 \\ 1 & 1 & 1 & -\lambda & 0 & 0 & 0 \\ 1 & 0 & 0 & 0 & -\lambda & 1 & 1 \\ 1 & 0 & 0 & 0 & 1 & -\lambda & 1 \\ 1 & 0 & 0 & 0 & 1 & 1 & -\lambda \end{bmatrix} \rightarrow \begin{bmatrix} -\lambda & 1 & 0 & 0 & 0 & 0 & 1 \\ 1 & -\lambda & 1+\lambda & 1+\lambda & 0 & 0 & 0 \\ 1 & 1 & -\lambda-1 & 0 & 0 & 0 & 0 \\ 1 & 1 & 0 & -\lambda-1 & 0 & 0 & 0 \\ 1 & 0 & 0 & 0 & -\lambda-1 & 0 & 1 \\ 1 & 0 & 0 & 0 & 0 & -\lambda-1 & 1 \\ 1 & 0 & 0 & 0 & 0 & 1+\lambda & 1+\lambda & -\lambda \end{bmatrix}$$

Next, we work on manipulating the rows of the new matrix. We perform the following operations: $R_2 + R_3 = R_2$; $R_2 + R_4 = R_2$; $R_7 + R_6 = R_7$; and, $R_7 + R_5 = R_7$.

$$\begin{bmatrix} -\lambda & 1 & 0 & 0 & 0 & 0 & 1 \\ 1 & -\lambda & 1+\lambda & 1+\lambda & 0 & 0 & 0 \\ 1 & 1 & -\lambda-1 & 0 & 0 & 0 & 0 \\ 1 & 1 & 0 & -\lambda-1 & 0 & 0 & 0 \\ 1 & 0 & 0 & 0 & -\lambda-1 & 0 & 1 \\ 1 & 0 & 0 & 0 & 0 & -\lambda-1 & 1 \\ 1 & 0 & 0 & 0 & 1+\lambda & 1+\lambda & -\lambda \end{bmatrix} \rightarrow \begin{bmatrix} -\lambda & 1 & 0 & 0 & 0 & 0 & 1 \\ 3 & 2-\lambda & 0 & 0 & 0 & 0 & 0 \\ 1 & 0 & -\lambda-1 & 0 & 0 & 0 & 0 \\ 1 & 0 & 0 & -\lambda-1 & 0 & 0 & 0 \\ 1 & 0 & 0 & 0 & -\lambda-1 & 0 & 1 \\ 1 & 0 & 0 & 0 & 0 & -\lambda-1 & 1 \\ 3 & 0 & 0 & 0 & 0 & 0 & 2-\lambda \end{bmatrix}$$

From here, we continue by changing the final rows $R_3 - R_1 = R_3$ and $R_4 - R_1 = R_4$, and then performing the final operation of $R_1 - (2-\lambda)R_2 = R_1$:

$$\begin{bmatrix} -\lambda & 1 & 0 & 0 & 0 & 0 & 1 \\ 3 & 2-\lambda & 0 & 0 & 0 & 0 & 0 \\ 1 & 0 & -\lambda-1 & 0 & 0 & 0 & 0 \\ 1 & 0 & 0 & -\lambda-1 & 0 & 0 & 0 \\ 1 & 0 & 0 & 0 & -\lambda-1 & 0 & 1 \\ 1 & 0 & 0 & 0 & 0 & -\lambda-1 & 1 \\ 3 & 0 & 0 & 0 & 0 & 0 & 2-\lambda \end{bmatrix} \rightarrow \begin{bmatrix} -\lambda - \frac{3}{2-\lambda} & 0 & 0 & 0 & 0 & 0 & 1 \\ 3 & 2-\lambda & 0 & 0 & 0 & 0 & 0 \\ 1+\lambda & 0 & -\lambda-1 & 0 & 0 & 0 & -1 \\ 1+\lambda & 0 & 0 & -\lambda-1 & 0 & 0 & -1 \\ 1 & 0 & 0 & 0 & -\lambda-1 & 0 & 1 \\ 1 & 0 & 0 & 0 & 0 & 0 & -\lambda-1 \\ 3 & 0 & 0 & 0 & 0 & 0 & 2-\lambda \end{bmatrix}$$

These results indicate that there is one $\lambda=2$ and four solutions of $\lambda=-1$.

For $\tau=3$, we do the same process:

$$\begin{bmatrix} -\lambda & 1 & 1 & 1 & 1 & 1 & 1 & 1 & 1 & 1 \\ 1 & -\lambda & 1 & 1 & 0 & 0 & 0 & 0 & 0 & 0 \\ 1 & 1 & -\lambda & 1 & 0 & 0 & 0 & 0 & 0 & 0 \\ 1 & 1 & 1 & -\lambda & 0 & 0 & 0 & 0 & 0 & 0 \\ 1 & 0 & 0 & 0 & -\lambda & 1 & 1 & 0 & 0 & 0 \\ 1 & 0 & 0 & 0 & 1 & -\lambda & 1 & 0 & 0 & 0 \\ 1 & 0 & 0 & 0 & 1 & 1 & -\lambda & 1 & 1 & 1 \\ 1 & 0 & 0 & 0 & 0 & 0 & 0 & -\lambda & 1 & 1 \\ 1 & 0 & 0 & 0 & 0 & 0 & 0 & 1 & -\lambda & 1 \\ 1 & 0 & 0 & 0 & 0 & 0 & 0 & 1 & 1 & -\lambda \end{bmatrix}$$

$$\rightarrow \begin{bmatrix} -\lambda - \frac{3}{2-\lambda} & 0 & 0 & 0 & 0 & 0 & 1 & 0 & 0 & 1 \\ 3 & 2-\lambda & 0 & 0 & 0 & 0 & 0 & 0 & 0 & 0 \\ 1+\lambda & 0 & -1-\lambda & 0 & 0 & 0 & 0 & 0 & 0 & 0 \\ 1+\lambda & 0 & 0 & -1-\lambda & 0 & 0 & 0 & 0 & 0 & 0 \\ 1 & 0 & 0 & 0 & -1-\lambda & 0 & 1 & 0 & 0 & 0 \\ 1 & 0 & 0 & 0 & 0 & -1-\lambda & 1 & 0 & 0 & 0 \\ 3 & 0 & 0 & 0 & 0 & 0 & 2-\lambda & 0 & 0 & 0 \\ 1 & 0 & 0 & 0 & 0 & 0 & 0 & -1-\lambda & 0 & 1 \\ 1 & 0 & 0 & 0 & 0 & 0 & 0 & 0 & -1-\lambda & 1 \\ 3 & 0 & 0 & 0 & 0 & 0 & 0 & 0 & 0 & 2-\lambda \end{bmatrix}$$

These results indicate that we can isolate $\lambda=2$ and 6 instances of $\lambda=-1$. We can generalize these matrices as follows:

$$\begin{bmatrix} -\lambda & 1 & 1 & \dots \\ 1 & K_3(-\lambda I) & 0 & \dots \\ 1 & 0 & \ddots & \dots \\ \vdots & \vdots & \dots & K_3(-\lambda I) \end{bmatrix}$$

where $K_3(-\lambda I)$ is a subset of the $K_4(-\lambda I)$ matrix such that

$$K_3(-\lambda I) = \begin{bmatrix} -\lambda & 1 & 1 \\ 1 & -\lambda & 1 \\ 1 & 1 & -\lambda \end{bmatrix}.$$

Therefore, we can assume these matrices to be true for some value of τ such that

$$\begin{bmatrix} -\lambda & 1 & 1 & 1 \\ 1 & K_3(-\lambda I) & 0 & 0 \\ 1 & 0 & K_3(-\lambda I) & 0 \\ 1 & 0 & 0 & \tau \end{bmatrix}$$

where τ is the $K_3(-\lambda I)$ subset of the number of K_4 subgraphs in the graph of interest. Next, we show this to be true for $\tau+1$ so that

$$\begin{bmatrix} -\lambda & 1 & 1 & 1 & 1 \\ 1 & K_3(-\lambda I) & 0 & 0 & 0 \\ 1 & 0 & K_3(-\lambda I) & 0 & 0 \\ 1 & 0 & 0 & \tau & 0 \\ 1 & 0 & 0 & 0 & \tau+1 \end{bmatrix}$$

From our assumption, we claim that we can isolate 2τ values of $-\lambda=-1$. Furthermore, we can isolate one $\lambda=2$ from our first K_4 matrix. If we are to determine the $\tau+1$ matrix, we should expect to isolate $2(\tau+1)=2\tau+2$ values of $\lambda=-1$.

Because three columns exist for each value of τ , and we utilize one column to isolate the two other columns, we are able to isolate two $\lambda=-1$, and unable to isolate the λ in the third column. Due to the extra column for $\tau=1$, we are able to isolate only one $\lambda=2$. As expected, for $\tau+1$, we are able to isolate $2\tau+2$ values of $\lambda=-1$.

Corollary 1. For the K_4 chain connected by single nodes, the maximum percentage of -1 eigenvalues is equivalent to $\frac{2}{3}$.

Proof.

As illustrated in Theorem 3, one can isolate at most two values of $\lambda = -1$ when $\tau > 1$ for each K_4 subgraph. Furthermore, in the corresponding $-1(\lambda \mathbf{I})$ matrix, three columns exist that represent each instance of τ , $\forall \tau > 1$. That said, 4 columns represent that particular subgraph for $\tau = 1$. Regardless, the assertion is that $\forall \tau$, one can isolate at most two columns of $\lambda = -1$. Therefore,

$$\sum \lambda^- = 2\tau$$

$$\sum \lambda^- = 4 + 3(\tau - 1)$$

This implies that

$$\frac{\lambda^-}{n} = \frac{2\tau}{4+3(\tau-1)} = \frac{2\tau}{4+3\tau-3} = \frac{2\tau}{1+3\tau}$$

As $\tau \rightarrow \infty$, then the percentage λ^- converges to $\frac{2}{3}$

$$\lim_{\tau \rightarrow \infty} \frac{2\tau}{1+3\tau} = \frac{2}{3}$$

C – Additional Links Attached to a Common Node

Theorem 4. For every m additional sets of nodes/links separately attached to a common node in a K_4 graph, $\lambda = 0$ occurs with multiplicity $m - 1$.

Proof.

We examine graphs composed of K_4 subgraphs and additional links (edges and nodes) attached to a common node in it. To begin, we focus on a graph composed of a single K_4 subgraph and additional nodes and edges, as illustrated in Figure 23.

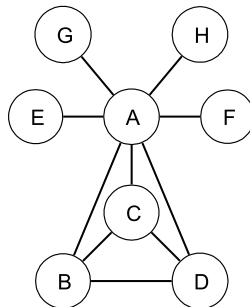


Fig. 23. Additional links attached to a common node

Let m be the number of additional links and nodes added to the K_4 subgraph. For $m=1$, the $\mathbf{A}-\lambda\mathbf{I}$ connectivity matrix is as follows:

$$\begin{bmatrix} -\lambda & 1 & 1 & 1 & 1 \\ 1 & -\lambda & 1 & 1 & 0 \\ 1 & 1 & -\lambda & 1 & 0 \\ 1 & 1 & 1 & -\lambda & 0 \\ 1 & 0 & 0 & 0 & -\lambda \end{bmatrix}.$$

Similar to the previous two proofs, we focus on isolating columns of this matrix by using row and column matrix operations:

$$\begin{bmatrix} -\lambda & 1 & 1 & 1 & 1 \\ 1 & -\lambda & 1 & 1 & 0 \\ 1 & 1 & -\lambda & 1 & 0 \\ 1 & 1 & 1 & -\lambda & 0 \\ 1 & 0 & 0 & 0 & -\lambda \end{bmatrix} \rightarrow \begin{bmatrix} -\lambda-1 & 0 & 0 & 1 & 1 \\ 0 & -\lambda-1 & 0 & 2 & 1 \\ 0 & 0 & -\lambda-1 & 3 & 1 \\ 0 & 0 & 0 & 3-\lambda & 1 \\ 1 & 0 & 0 & 0 & -\lambda \end{bmatrix}.$$

In this instance, we cannot isolate any values of λ equal to zero; however, we can isolate two instances of $\lambda=-1$ from the K_4 subgraph. This supports our theorem, as we would expect the number of $\lambda=0$ to be $m-1=1-1=0$.

For $m=2$, we follow the same process concerning λ -values with row and column operations:

$$\begin{bmatrix} -\lambda & 1 & 1 & 1 & 1 & 1 \\ 1 & -\lambda & 1 & 1 & 0 & 0 \\ 1 & 1 & -\lambda & 1 & 0 & 0 \\ 1 & 1 & 1 & -\lambda & 0 & 0 \\ 1 & 0 & 0 & 0 & -\lambda & 0 \\ 1 & 0 & 0 & 0 & 0 & -\lambda \end{bmatrix} \rightarrow \begin{bmatrix} -\lambda-1 & 0 & 0 & 1 & 1 & 0 \\ 0 & -\lambda-1 & 0 & 2 & 1 & 0 \\ 0 & 0 & -\lambda-1 & 3 & 1 & 0 \\ 0 & 0 & 0 & 3-\lambda & 1 & 0 \\ 2 & 0 & 0 & 0 & -\lambda & 0 \\ 1 & 0 & 0 & 0 & 0 & -\lambda \end{bmatrix}.$$

In this case, we can isolate one $\lambda=0$, and in doing so, maintain the other columns that we previously isolated.

Again, for $m=3$, we follow the same process:

$$\begin{bmatrix} -\lambda & 1 & 1 & 1 & 1 & 1 & 1 \\ 1 & -\lambda & 1 & 1 & 0 & 0 & 0 \\ 1 & 1 & -\lambda & 1 & 0 & 0 & 0 \\ 1 & 1 & 1 & -\lambda & 0 & 0 & 0 \\ 1 & 0 & 0 & 0 & -\lambda & 0 & 0 \\ 1 & 0 & 0 & 0 & 0 & -\lambda & 0 \\ 1 & 0 & 0 & 0 & 0 & 0 & -\lambda \end{bmatrix} \rightarrow \begin{bmatrix} -\lambda-1 & 0 & 0 & 1 & 1 & 0 & 0 \\ 0 & -\lambda-1 & 0 & 2 & 1 & 0 & 0 \\ 0 & 0 & -\lambda-1 & 3 & 1 & 0 & 0 \\ 0 & 0 & 0 & 3-\lambda & 1 & 0 & 0 \\ 3 & 0 & 0 & 0 & -\lambda & 0 & 0 \\ 2 & 0 & 0 & 0 & 0 & -\lambda & 0 \\ 1 & 0 & 0 & 0 & 0 & 0 & -\lambda \end{bmatrix}.$$

Notice now that we isolate two instances of $\lambda=0$, while still maintaining the previous isolated λ -values of the remainder of the graph, with the exception of the additional edges. Furthermore, notice that for the previous examples, the only elements that change values when attempting to isolate the columns of the additional nodes are the elements of those columns, as well as the elements of column 1 associated with the aforementioned columns.

These elements in column 1 are denoted **in blue** in the previous three matrices.

Let \mathbf{S} be the subgraph $\mathbf{A}-\lambda\mathbf{I}$ matrix that *does not* include the additional node row/columns. As shown for K_4+1 , K_4+2 , and K_4+3 , we *always* can isolate the possible columns of \mathbf{S} , regardless of the size of m , with the additional nodes separately attached to the common node; these additional nodes only affect row and column 1, with their remaining elements being zero. We cannot isolate $m=1$ because it is needed to rearrange the other m -columns to isolate $\lambda=0$.

Now, let $m=k$, where k is an arbitrary number of additional edges. Then, the respective $\mathbf{A}-\lambda\mathbf{I}$ matrix is of the form

$$\begin{bmatrix} \mathbf{S} & 1_{i=1} & 1_{i=2} & \cdots & 1_{i=k} \\ 1_{i=1} & -\lambda_{i=1} & 0 & \cdots & 0 \\ 1_{i=2} & 0 & -\lambda_{i=2} & 0 & 0 \\ \vdots & 0 & 0 & \ddots & \vdots \\ 1_{i=k} & 0 & \cdots & 0 & -\lambda_{i=k} \end{bmatrix},$$

where \mathbf{S} is the adjacency matrix for the graph *without* the additional nodes. As before, isolating the columns through column and row matrix operations, the new matrix becomes

$$\begin{bmatrix} \mathbf{S} & 1_{i=1} & 0_{i=2} & \cdots & 0_{i=k} \\ k & -\lambda_{i=1} & 0 & \cdots & 0 \\ k-1 & 0 & -\lambda_{i=2} & \ddots & \vdots \\ k-2 & 0 & 0 & -\lambda_{i=3} & 0 \\ \vdots & \vdots & 0 & \ddots & \vdots \\ 1_{i=k} & 0 & \cdots & \cdots & -\lambda_{i=k} \end{bmatrix}.$$

We can isolate $k-1$ additional edges, again leaving $m=1$ to help isolate the subsequent columns. Note that the \mathbf{S} component of the matrix ultimately expands this matrix, in this example expanding it by three rows/columns, because the first row of the K_4 subgraph is included in the pre-existing matrix. Furthermore, note how the elements of column 1 decrease from k to 1 after the last element of the \mathbf{S} matrix.

This matrix can be extended to an arbitrarily large size, and the process remains the same.

prof. Daniel A. Griffith, Nicholas P. Taliceo

School of Economic, Political and Policy Sciences

University of Texas at Dallas, USA

800 W. Campbell Rd

Richardson, Texas 75080-3021

dagriffith@utdallas.edu, Nicholas.Taliceo@utdallas.edu